

Infrared Reflectivity Spectra of the Mixed Crystal System  $\text{Ga}_{1-x}\text{In}_x\text{Sb}^\dagger$ 

M. H. Brodsky

*IBM Thomas J. Watson Research Center, Yorktown Heights, New York 10598*

and

G. Lucovsky

*Xerox Corporation, Rochester, New York 14603*

and

M. F. Chen

*University of Rochester, Rochester, New York 14627*

and

T. S. Plaskett

*IBM Thomas J. Watson Research Center, Yorktown Heights, New York 10598*

(Received 20 April 1970)

We report measurements of the far-infrared reflectivity spectra for the pseudobinary system  $\text{Ga}_{1-x}\text{In}_x\text{Sb}$ . Data were analyzed with a Kramers-Kronig dispersion analysis and a damped Lorentzian oscillator formalism. For  $x < 0.30$ , one TO-phonon mode is evident, whereas for  $x > 0.30$ , two TO modes are observed. The variations of the TO-phonon frequencies and the mode strengths do not conform to the traditional types of behavior previously used to describe the long-wavelength optical phonons in pseudobinary alloy systems. An alternative classification scheme, based on the occurrence of gap and/or local modes, is proposed. It is sufficiently general to encompass the previously defined classes of behavior, as well as the behavior we report here for the  $\text{Ga}_{1-x}\text{In}_x\text{Sb}$  system.

## I. INTRODUCTION

The work reported here forms part of a continuing study<sup>1,2</sup> of the long-wavelength optical lattice vibrations in pseudobinary mixed crystals of the form  $A_{1-x}B_xC$ . Workers in this field have traditionally classified their observations of optical phonons as being representative of either one- or two-mode behavior.<sup>3</sup> One-mode behavior has been defined by the occurrence of one strong transverse-optical (TO) phonon mode over the entire composition range ( $1 \geq x \geq 0$ ). The frequency and oscillator strength of this mode vary continuously between those of the end member compounds,  $AC$  and  $BC$ . This type of behavior has been reported in  $\text{Na}_{1-x}\text{K}_x\text{Cl}$ ,<sup>4</sup>  $\text{KCl}_{1-x}\text{Br}_x$ ,<sup>5</sup> several other alkali halide mixtures,<sup>4,6</sup>  $\text{Ni}_{1-x}\text{Co}_x\text{O}$ ,<sup>7</sup>  $\text{Zn}_{1-x}\text{Cd}_x\text{S}$ ,<sup>8</sup> and  $\text{ZnSe}_{1-x}\text{Te}_x$ .<sup>9</sup> Two-mode behavior has been defined by the occurrence of two dominant TO modes. One occurs at approximately the TO-phonon frequency of  $AC$  with an oscillator strength that decreases as  $x$  increases, and the other occurs at approximately the TO-phonon frequency of  $BC$  with an oscillator strength that increases as  $x$  increases. Examples of this type of behavior have been reported in  $\text{GaP}_{1-x}\text{As}_x$ ,<sup>10,11</sup>  $\text{CdS}_{1-x}\text{Se}_x$ ,<sup>12-15</sup> and  $\text{Al}_{1-x}\text{Ga}_x\text{As}$ .<sup>16</sup> In addition to these dominant characteristics, other very weak modes have also been reported<sup>8,10</sup> in both one- and two-mode systems. Brodsky and Lucovsky<sup>2</sup> studied the infrared-active modes in  $\text{Ga}_{1-x}\text{In}_x\text{As}$  and found that they could not simply classify their results in the usual sense as defined above. Whereas the TO-phonon frequency of the

low-frequency mode was approximately equal to the TO-phonon frequency of  $\text{InAs}$ , the frequency of the second TO mode varied from the TO frequency of  $\text{GaAs}$  ( $268 \text{ cm}^{-1}$ ) at  $x=0$  to close to the LO frequency of  $\text{InAs}$  ( $\sim 240 \text{ cm}^{-1}$ ) for  $x=1$ .

In this paper, we report and discuss the room-temperature reflectivity spectra of  $\text{Ga}_{1-x}\text{In}_x\text{Sb}$  mixed crystals. The spectra obtained are similar to those reported for  $\text{Ga}_{1-x}\text{In}_x\text{As}$  and have helped to clarify the generality of the nature of two-mode behavior and to define the criteria for its occurrence. Lucovsky, Brodsky, and Burstein<sup>1</sup> discussed various models that have been used to interpret the behavior with composition of the long-wavelength optical phonons in mixed crystals and put forth criteria for the occurrence of two-mode behavior. They suggested that two-mode behavior would occur for all  $x$  if (1) the substitution of  $A$  for  $B$  in  $BC$  produced a local mode and (2) the substitution of  $B$  for  $A$  in  $AC$  produced a gap mode. We have assumed a notation where the mass of  $B$  is greater than the mass of  $A$ . The behavior reported here as well as the results in  $\text{Ga}_{1-x}\text{In}_x\text{As}$  indicate that the criteria for local and gap modes should be considered separately, i.e., two-mode behavior can occur over only part of the composition range if either the gap- or local-mode condition is satisfied but the other is not.

In Sec. II, we discuss the experimental details describing the sample preparation and characterization as well as the reflectivity measurements. The data and the results of the Kramers-Kronig and Lorentzian oscillator analyses are presented

in Sec. III. Section IV discusses our results in terms of a set of newly proposed categories which relate mixed crystal behavior to impurity mode behavior. We also indicate how other systems which have been studied can be fitted into our classification scheme. Section V summarizes our conclusions.

## II. EXPERIMENTAL PROCEDURES

The samples used in these studies were cut from polycrystalline melt-grown ingots. The end member compounds, GaSb and InSb, were synthesized from the elements and given a two-pass zone-refining treatment. Mixed crystal ingots were prepared from the zone-refined compounds by zone leveling an ingot of the desired composition. A zone travel rate of 1 mm/hr provided single-phase large-grained polycrystalline material of uniform composition. The composition of a sample was determined by a measurement of the band gap by optical absorption. The sharp absorption edges observed were an indication of homogeneous samples. Homogeneity and composition were further verified for selected samples by x-ray diffraction. Room-temperature measurements of the Hall constant indicated, for compositions up to  $x \approx 0.5$  (50% InSb), that the mixed crystals were  $p$  type, whereas for compositions with  $x > 0.5$ , they were  $n$  type. The carrier concentrations were sufficiently low to ensure that the free-carrier plasma mode frequencies were well below the lowest lattice mode frequencies of interest.

Wafers, cut from the ingots, were chemically polished on a rotating Pellon cloth which was continually saturated with a solution of  $\text{Cl}_2$  in methanol. The amount of  $\text{Cl}_2$  in solution was varied with alloy composition in order to give a high-quality polished surface.

The reflection spectra were taken at room temperature using a Perkin-Elmer model 301 spectrometer. The spectral range studied was 135–285  $\text{cm}^{-1}$ ; 10- and 20-line/mm gratings were used in first order. Calibration was accomplished using known water absorption bands. The spectrometer was operated in a single-beam mode and the reflectances of the samples were compared to that of a front-surface Al-coated mirror. Spectral resolution was of the order of 1–2  $\text{cm}^{-1}$ .

## III. EXPERIMENTAL RESULTS AND ANALYSIS

### A. Experimental Results

Figure 1 contains the reflectivity spectra of the eight  $\text{Ga}_{1-x}\text{In}_x\text{Sb}$  samples studied. Also included are spectra for the end member compounds, GaSb and InSb. The behavior reported here parallels that previously reported for the system  $\text{Ga}_{1-x}\text{In}_x\text{As}$ .<sup>2</sup> Two reflectance bands are clearly evident for those

alloy samples with  $x > 0.3$ . No fine structure, as reported for example in  $\text{GaP}_{1-x}\text{As}_x$ ,<sup>10,11</sup> is evident. As  $x$  is increased the high-frequency band shifts downward in frequency out of the GaSb reststrahlen region and approaches, in the  $x = 0.95$  sample, the high-frequency limit of the InSb reststrahlen band. On the other hand, with the exception of the  $x = 0.30$  sample, the low-frequency band falls within the InSb reststrahlen band for all compositions. The position of the low-frequency band in the  $x = 0.30$  sample makes us question whether it results from the same mechanism as the low-frequency band in the other samples. We believe that this structure is real because it was observable in two separate samples cut from different ingots.

### B. Dispersion Analysis of Reflectance

The reflectivity spectra were first analyzed using a Kramers-Kronig (KK) dispersion analysis. TO-phonon frequencies  $\omega_{\text{TO}}(i)$  were estimated from the

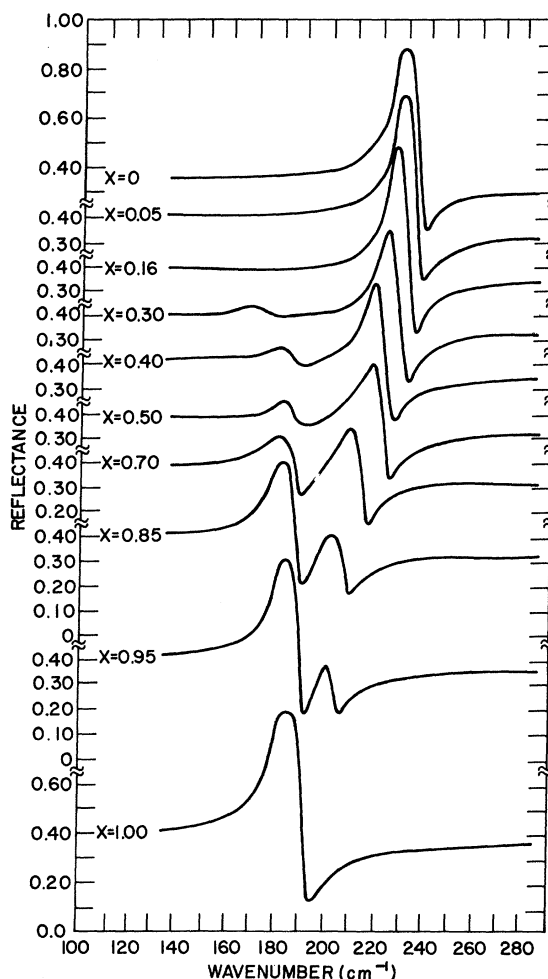


FIG. 1. Reflectances as a function wave number for the alloy system  $\text{Ga}_{1-x}\text{In}_x\text{Sb}$ .

TABLE I. Oscillator parameters and phonon frequencies for the system  $\text{Ga}_{1-x}\text{In}_x\text{Sb}$  as derived from Kramers-Kronig analysis and from damped Lorentzian oscillator fits.

Alloy composition	Kramers-Kronig analysis					Lorentzian oscillator analysis						
	$\omega_{\text{TO}}(1)$ ( $\text{cm}^{-1}$ )	$\omega_{\text{LO}}(1)$ ( $\text{cm}^{-1}$ )	$\omega_{\text{LO}}(1)$ ( $\text{cm}^{-1}$ )	$\omega_{\text{LO}}(2)$ ( $\text{cm}^{-1}$ )	$\omega_{\text{TO}}(1)$ ( $\text{cm}^{-1}$ )	$S_1$	$\gamma_1$	$\omega_{\text{LO}}(1)$ ( $\text{cm}^{-1}$ )	$\omega_{\text{TO}}(2)$ ( $\text{cm}^{-1}$ )	$S_2$	$\gamma_2$	$\omega_{\text{LO}}(2)$ ( $\text{cm}^{-1}$ )
GaSb	227	237	...	...	227	1.45	0.010	238	...	...	...	...
$\text{Ga}_{0.95}\text{In}_{0.05}\text{Sb}$	226	237	...	...	226	1.61	0.010	236	...	...	...	...
$\text{Ga}_{0.84}\text{In}_{0.16}\text{Sb}$	224	233	...	...	224	1.41	0.011	233	...	...	...	...
$\text{Ga}_{0.70}\text{In}_{0.30}\text{Sb}$	221	230	174	175	221	1.33	0.019	230	175	0.160	0.025	176
$\text{Ga}_{0.60}\text{In}_{0.40}\text{Sb}$	217	225	183	186	217	1.27	0.017	225	184	0.560	0.055	186
$\text{Ga}_{0.50}\text{In}_{0.50}\text{Sb}$	215	223	183	186	215	1.00	0.024	223	184	0.47	0.046	186
$\text{Ga}_{0.30}\text{In}_{0.70}\text{Sb}$	207	214	180	187	208	0.75	0.026	214	181	1.00	0.042	186
$\text{Ga}_{0.15}\text{In}_{0.85}\text{Sb}$	201	207	178	188	202	0.47	0.032	207	179	1.90	0.024	188
$\text{Ga}_{0.05}\text{In}_{0.95}\text{Sb}$	201	204	180	190	201	0.27	0.024	204	181	2.22	0.016	191
InSb	...	...	180	193	...	...	...	...	180	2.64	0.014	193

positions of the relative maxima in the imaginary part of the dielectric constant  $\epsilon_2$ , and LO-phonon frequencies  $\omega_{\text{LO}}(i)$  were estimated from the positions of the maxima in the energy-loss term  $-\text{Im}(1/\epsilon)$ . These are included in Table I, where the index  $i=1$  identifies parameters characterizing the high-frequency band and the index  $i=2$  identifies the low-frequency band parameters. The  $\omega_{\text{TO}}(i)$  along with mode strengths  $S_i$ , and damping parameters  $\gamma_i$  as estimated from the KK analysis were used as starting values in a damped Lorentzian oscillator formalism to synthesize a reflectivity spectrum.<sup>17</sup> Using two oscillators that contribute to the dielectric constant according to

$$\epsilon(\omega) = \epsilon_\infty + \sum_{i=1}^2 \frac{S_i \omega_{\text{TO}}^2(i)}{\omega_{\text{TO}}^2(i) - \omega^2 - i\gamma_i \omega_{\text{TO}}(i)\omega},$$

the parameters were adjusted until a good fit was obtained between the synthesized and experimental reflectivity. As pointed out above, the plasma

frequencies were sufficiently low to ensure that the reststrahlen bands were well isolated from the plasma edge. The onset of interband electronic transitions was well removed to higher frequencies. These conditions ensure that the parameters derived from the KK analysis are good starting values for an oscillator fit of the reflectivity. Figures 2-9 display the synthesized and experimental reflectances of the alloy samples,  $x=0.05-0.95$ . In Table I we give the oscillator parameters for each composition, and also include the values of the LO-phonon frequencies as determined from the positions of the maxima in  $-\text{Im}(1/\epsilon)$  in the synthesized dielectric constant. For reasons indicated above, the phonon frequencies as obtained from the KK analysis and oscillator analysis are in good agreement with each other.

Figure 10 contains a plot of the compositional dependence of the TO- and LO-phonon frequencies as obtained from the oscillator analysis. First consider the variation of the TO-phonon frequencies.

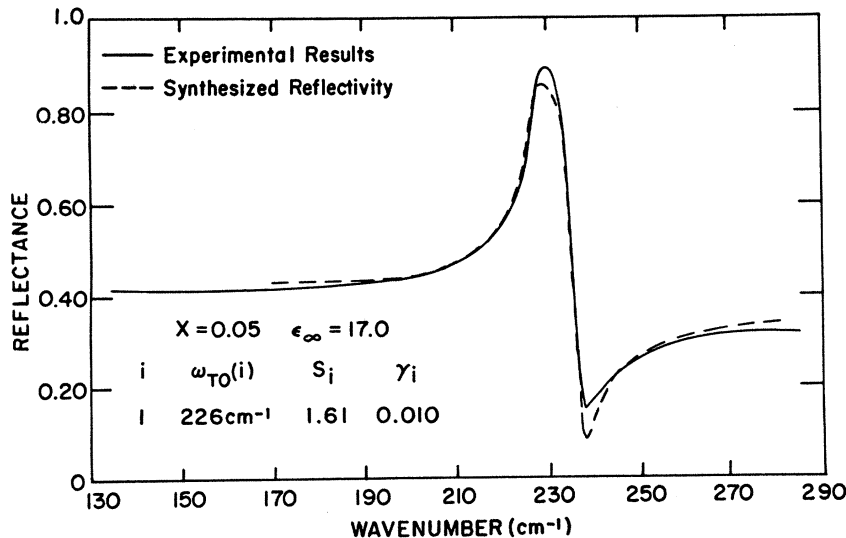


FIG. 2. Theoretical fit to experimental reflectivity data for  $x=0.05$ . The oscillator parameters and high-frequency dielectric constant  $\epsilon_\infty$  are shown in the figure.

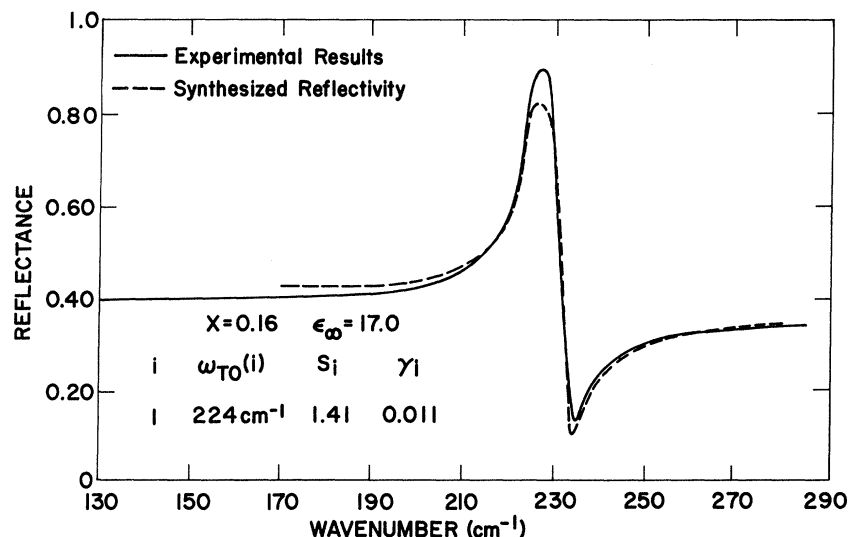


FIG. 3. Theoretical fit to experimental reflectivity data for  $x=0.16$ . The oscillator parameters and high-frequency dielectric constant  $\epsilon_\infty$  are shown in the figure.

For the high-frequency band, the dependence can be approximated by two linear regions; for small concentrations of In in GaSb ( $x < 0.3$ ), the "GaSb-like" mode frequency decreases less rapidly with  $x$  than it does for larger concentrations ( $x > 0.3$ ). The extrapolated value of the local-mode frequency of Ga in InSb is 199 cm<sup>-1</sup>. The variation of the low-frequency TO-phonon frequency with composition is also essentially linear but with much less steep a slope. For both the high- and low-frequency branches the variation of the LO-phonon frequencies is monotonic with  $x$ , but nonlinear because of mode coupling by long-range forces.

Figure 11(a) contains a plot of the oscillator strength parameters for the two modes. For the high-frequency branch the oscillator strength decreases slowly for  $x < 0.4$  and then falls off much

more rapidly, extrapolating to a value  $\sim 0.15$  for  $x=1.0$ . This value of the oscillator strength of the local mode is similar to that reported by Verleur and Barker for the local mode of  $P$  in GaAs.<sup>10</sup> For the low-frequency branch, as  $x$  decreases, the oscillator strength decreases and extrapolates to a value of zero for  $x \sim 0.3$ .

Figure 11(b) displays the variation of the damping parameters,  $\gamma_i(x)$ , with composition.

#### IV. DISCUSSION

The variations of the TO-phonon frequencies  $\omega_{TO}(i)$  and the oscillator strengths  $S_i$  with composition do not conform to those of traditionally defined two-mode systems. Specifically, when compared to two-mode *prototype* systems — e.g., CdS<sub>1-x</sub>Se<sub>x</sub> or GaP<sub>1-x</sub>As<sub>x</sub> — the different features are

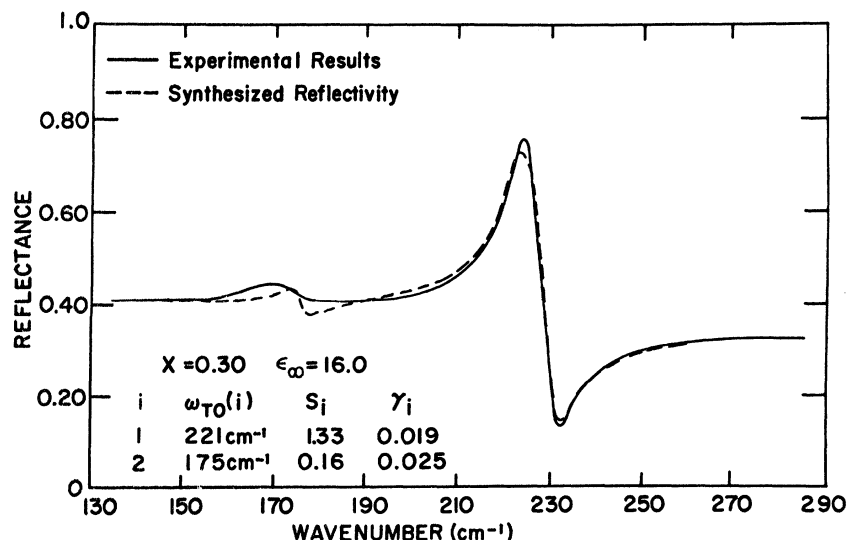


FIG. 4. Theoretical fit to experimental reflectivity data for  $x=0.30$ . The oscillator parameters and high-frequency dielectric constant  $\epsilon_\infty$  are shown in the figure.

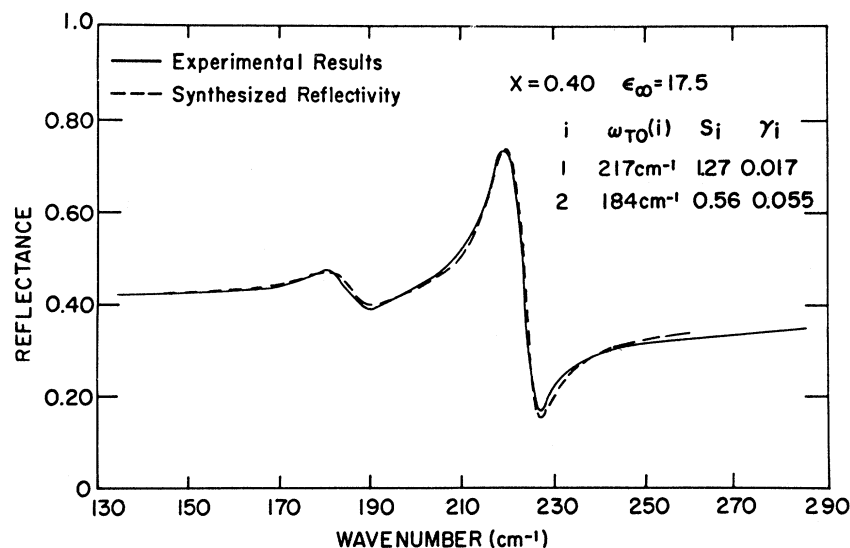


FIG. 5. Theoretical fit to experimental reflectivity data for  $x=0.40$ . The oscillator parameters and high-frequency dielectric constant  $\epsilon_\infty$  are shown in the figure.

as follows:

(i) Mode (2), the low-frequency mode, is only observable for  $x > 0.3$ ; there is still a question regarding the origin of the second mode in the  $x=0.3$  sample. The decrease of the oscillator strength of the low-frequency mode with decreasing  $x$  extrapolates to a value of zero at about  $x=0.3$ .

(ii) The TO-phonon frequency of the high-frequency mode, mode (1), differs significantly from the TO-phonon frequency for GaSb for  $x > 0.3$ . This is much clearer here than in  $\text{GaP}_{1-x}\text{As}_x$ , for example, where the frequency of the corresponding mode drops from 366 cm<sup>-1</sup> [TO(GaP)] to ~352 cm<sup>-1</sup> (local-mode frequency of P in GaAs) or approximately 4%, whereas in  $\text{Ga}_{1-x}\text{In}_x\text{Sb}$  the TO-phonon

frequency of mode (2) drops by approximately 11%. The difference arises because of the different local-mode frequencies. In general, for a system  $A_{1-x}B_xC$ , the local-mode frequency of A in BC is not necessarily close to the TO frequency of AC.<sup>18</sup>

We now propose a classification scheme based on the behavior of impurities at either end of the alloy composition range. This classification helps to define better the general nature of two-mode behavior as it is manifested in  $\text{Ga}_{1-x}\text{In}_x\text{Sb}$  and other systems. We propose a point of view that divides the observations of mixed crystal behavior into three categories. We are here concerned with the gross features of the system, i.e., the number of dominant modes and their variation in frequency

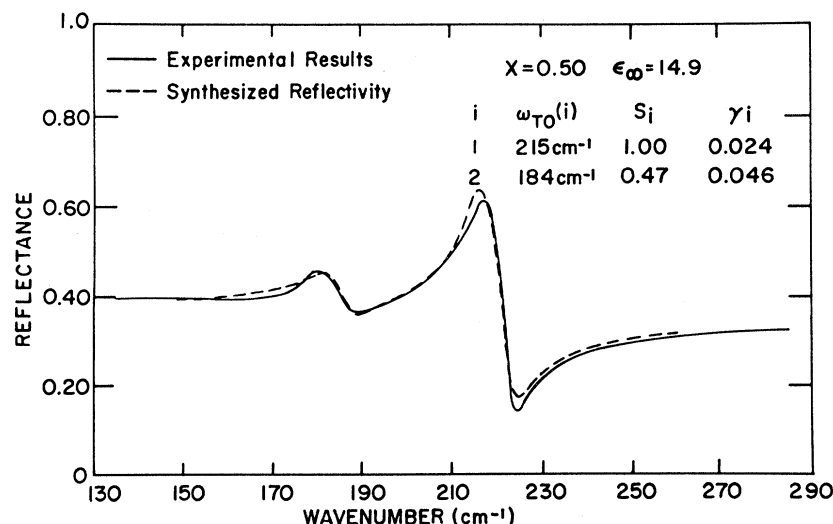


FIG. 6. Theoretical fit to experimental reflectivity data for  $x=0.50$ . The oscillator parameters and high-frequency dielectric constant  $\epsilon_\infty$  are shown in the figure.

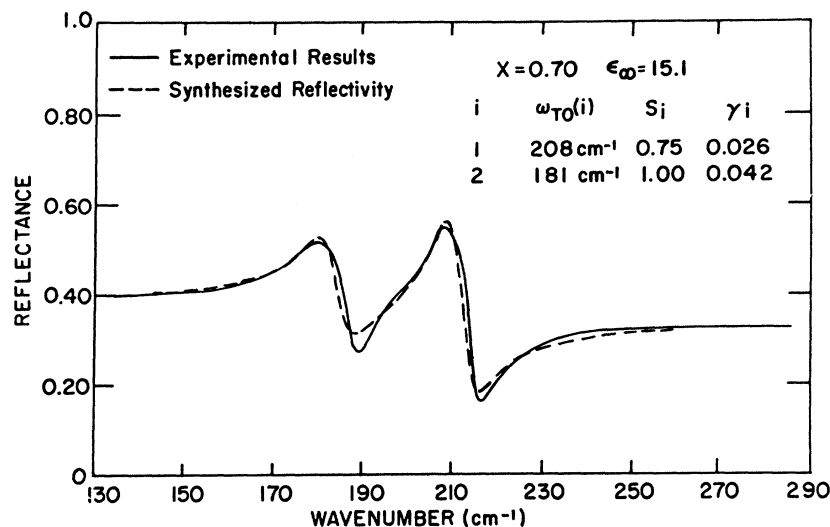


FIG. 7. Theoretical fit to experimental reflectivity data for  $x=0.70$ . The oscillator parameters and high-frequency dielectric constant  $\epsilon_\infty$  are shown in the figure.

and oscillator strength (for the TO modes only) with composition. A simple counting of the normal modes of vibration tells us that there are always two pairs of LO-TO branches for all values of  $x$  in the type of pseudobinary systems considered here,<sup>19</sup> but often in practice only one of these is observable. Therefore in a broad sense, each of the categories we define is a particular kind of manifestation of the general multimode system. The classification is made on the basis of the occurrence or nonoccurrence of either gap and/or localized modes in the limits of  $x$  near 0 and 1, respectively.

(1) The first category is the simplest to define and to understand. It is the case where both gap and local modes occur at the respective ends of the

alloy system. For this case two-mode behavior occurs for all  $x$ . The variation of the transverse frequencies with composition is well approximated by a linear extrapolation between the impurity mode frequencies and their respective end member TO-phonon frequencies. The point emphasized here is that the variation of frequency with composition is determined by the frequencies of the end member impurity modes,<sup>18</sup> which are not necessarily close to the TO-phonon frequencies of the appropriate end member compounds. In fact, for III-V materials, local-mode frequencies are always lower than the appropriate TO-phonon frequencies,<sup>10,11,16,18</sup> whereas in the II-VI materials they are always higher.<sup>12-15,18</sup> Therefore, for systems in this first category, the traditional definition of two-mode

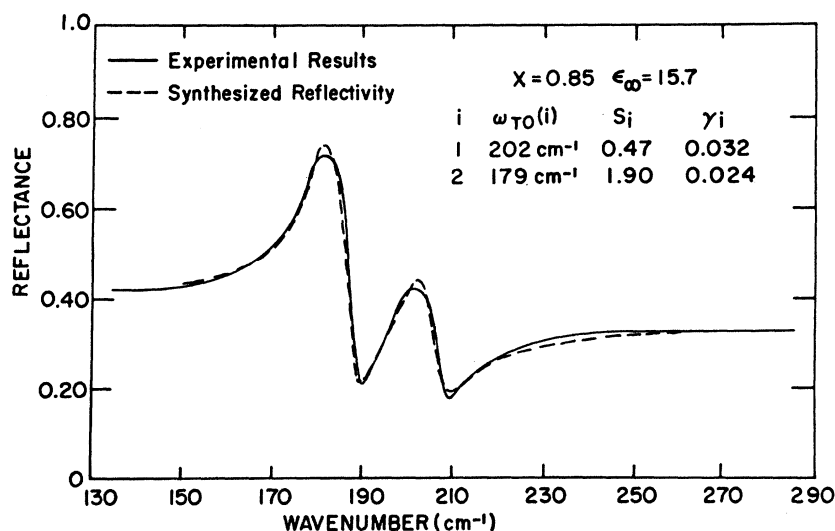


FIG. 8. Theoretical fit to experimental reflectivity data for  $x=0.85$ . The oscillator parameters and high-frequency dielectric constant  $\epsilon_\infty$  are shown in the figure.

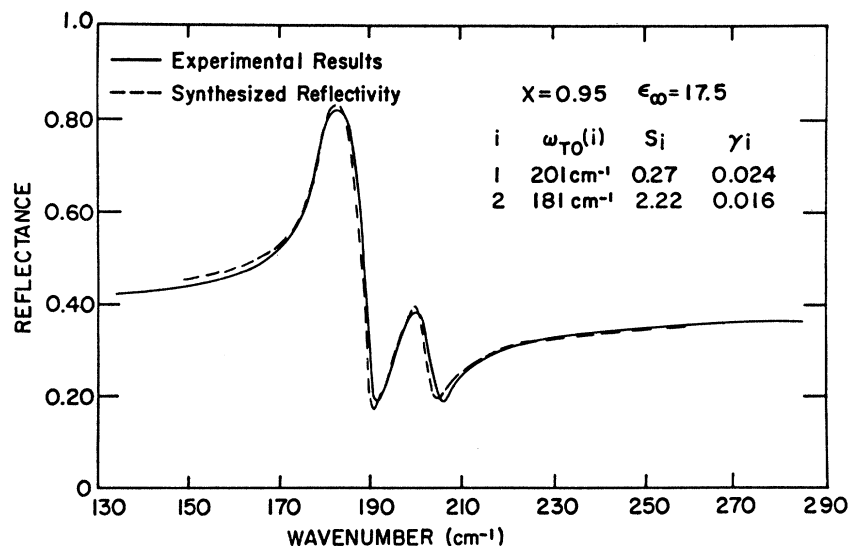


FIG. 9. Theoretical fit to experimental reflectivity data for  $x=0.95$ . The oscillator parameters and high-frequency dielectric constant  $\epsilon_\infty$  are shown in the figure.

behavior as given in the Introduction is too restrictive in the sense that the high-frequency mode need not have the same frequency as the light constituent of the mixture.

(2) The second category is one in which either the gap or local mode is allowed, but not both. In general, although not always, this leads to two-mode behavior over only a part of the composition range. If the gap mode is not allowed, e.g., because of the lack of a gap in the appropriate end member or because of mass considerations, then two-mode behavior occurs for large values of  $x$ . However, if the gap mode is the allowed mode, we expect two-mode behavior for small values of  $x$ . The nonlocal or nongap impurity mode is generally degenerate with phonon modes of the host crystal, and may not be observable depending on the degree of damping.

(3) The third category is one in which neither local nor gap modes are allowed. This leads to a single dominant TO-phonon mode, whose frequency and oscillator strength vary smoothly between those of the end member compounds.

Figure 12 illustrates schematically the phonon modes that occur for these three cases of impurity mode behavior. The results we presented here for  $\text{Ga}_{1-x}\text{In}_x\text{Sb}$  and the earlier results for  $\text{Ga}_{1-x}\text{In}_x\text{As}^2$  are representative of category (2) behavior in which the local mode is allowed and the gap mode not allowed. These results are consistent with a mass-defect calculation based on a modified linear diatomic-chain model which includes some relevant three-dimensional effects.<sup>18</sup> The model predicts that a local mode will be produced by the substitution of Ga for In in InSb. On the basis of the model

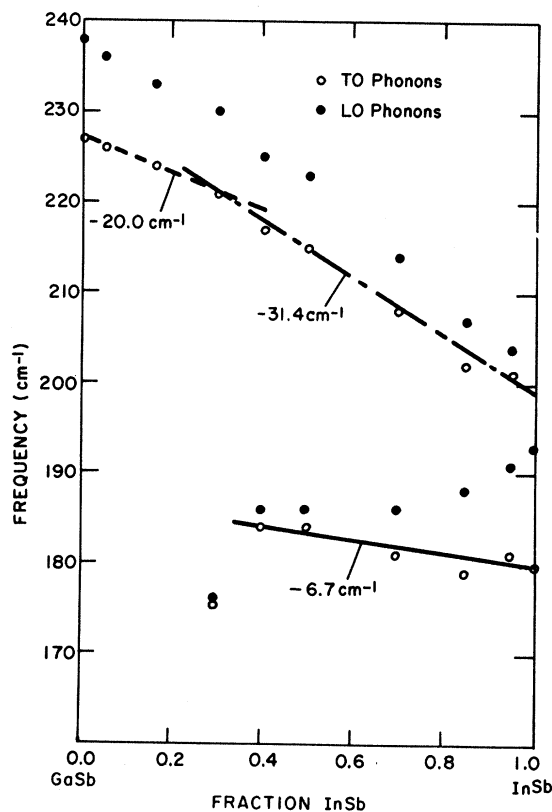


FIG. 10. Compositional dependence of the LO- and TO-phonon frequencies for  $\text{Ga}_{1-x}\text{In}_x\text{Sb}$  as deduced from the oscillator fit analysis. The points are derived from the data analysis. The lines are drawn to emphasize trends in the data points. The slopes  $d\gamma/dx$  are indicated.

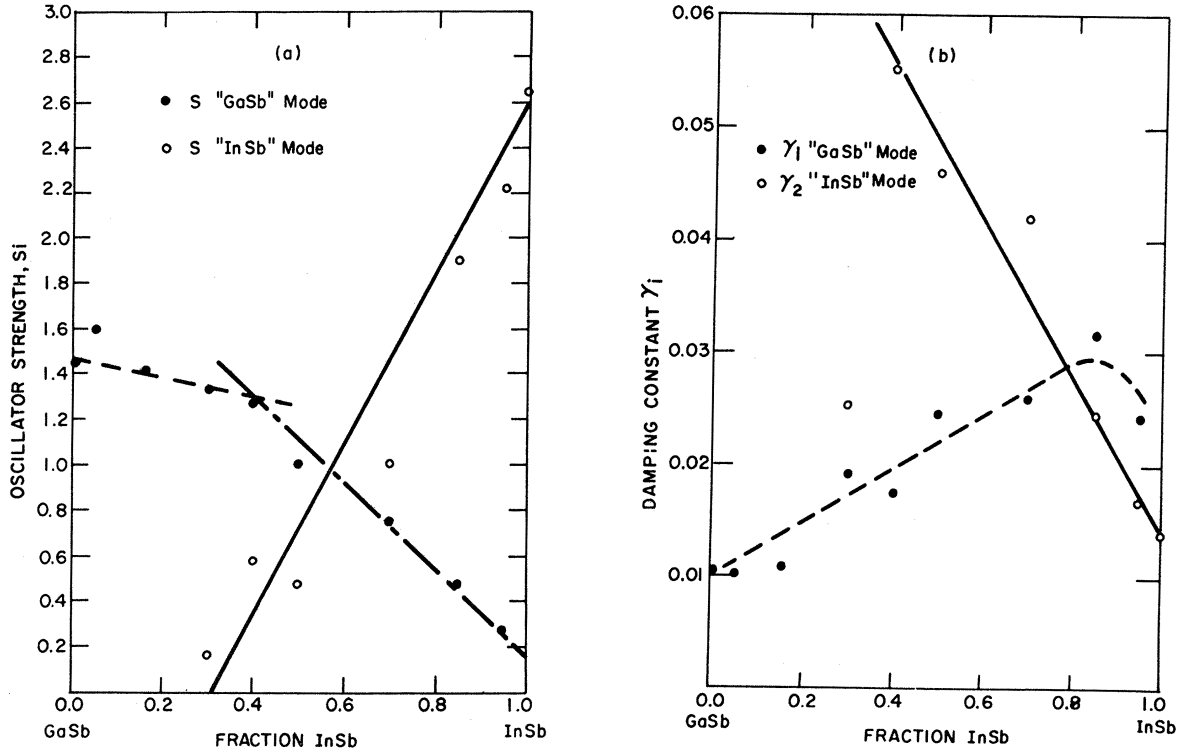


FIG. 11. (a) Compositional dependence of the oscillator strengths for  $\text{Ga}_{1-x}\text{In}_x\text{Sb}$  as deduced from the oscillator fit analysis. The points are derived from the data analysis. The lines are drawn to emphasize trends in the data points. (b) Compositional dependence of the damping parameters for  $\text{Ga}_{1-x}\text{In}_x\text{Sb}$  as deduced from oscillator fit analysis. The points are derived from the data analysis. The lines are drawn to emphasize trends in the data points.

we expect similar behavior in  $\text{GaAs}_{1-x}\text{Sb}_x$  and  $\text{InAs}_{1-x}\text{Sb}_x$ .<sup>20</sup> There is insufficient information about the phonon dispersion curves of GaSb to ascertain if there is a gap between the acoustical and optical branches of that crystal. The results of our experiment suggest that either no gap exists, or that if one does exist the impurity mode of In in GaSb, which from mass considerations must lie below the TO-phonon frequency of GaSb, is degenerate with phonon modes of GaSb and sufficiently damped to prevent its observation. The variations of oscillator strength and damping for mode (2) support our classification of the  $\text{Ga}_{1-x}\text{In}_x\text{Sb}$  system. In the categorization procedure, the reason that a gap mode is not observed is that the impurity mode produced by In in GaSb is degenerate in frequency with phonons of the GaSb host. This produces a strong coupling of the impurity mode to the host, which decreases its oscillator strength and also produces significant damping. The decrease in  $S_2$  and increase in  $\gamma_2$  with decreasing  $x$  are in agreement with our model.

Another interesting aspect of this mechanism is the effect of the low-frequency mode coming out of a band on the oscillator strength and frequency of

the high-frequency band. Note that near  $x \sim 0.30$  both of these parameters,  $\omega_{\text{TO}}(1)$  and  $S_1$ , show a change in their dependence on composition. As long as mode (2) is not observable, the oscillator strength of mode (1) varies slowly; as soon as mode (2) becomes observable the oscillator strength in mode (1) starts to drop more rapidly. The behavior of the oscillator strengths for  $x > 0.3$  is

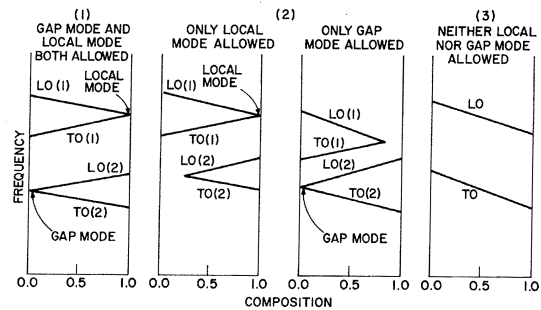


FIG. 12. Schematic representation of the compositional dependence in mixing crystal systems using a classification scheme based on local- and gap-mode occurrence at  $x = 0$  and  $x = 1$ .



similar to that of two-mode systems.

The systems discussed in the Introduction are associated with either one- or two-mode behavior in the traditional sense, and correspond, respectively, to categories (3) and (1) in our classification scheme. The results for  $K_{1-x}Rb_xI$  as reported by Fertel and Perry<sup>5</sup> are an interesting example of category (2) behavior. A gap mode is produced when Rb is added to KI; however, the impurity mode of K in RbI falls in the LO-TO reststrahlen region of RbI and as such is not a local mode.<sup>18</sup> However, presumably owing to the low density of states in the region of this impurity mode, it is not heavily damped and therefore is observable.

#### V. CONCLUSIONS

In summary, we have reported the infrared reflectivity for the pseudobinary mixed crystal system  $Ga_{1-x}In_xSb$ . We have analyzed the reflectivity data and have interpreted the spectra in terms of

a damped harmonic-oscillator model. The variation of the TO-phonon frequencies  $\omega_{TO}(z)$  with composition as well as the variation of their oscillator strengths  $S_i$  with composition do not conform to the traditional types of behavior defining the long-wavelength optical phonons in these pseudobinary alloys. We have proposed an alternative classification scheme, which includes the traditionally defined behavior but is general enough to encompass the behavior we report for  $Ga_{1-x}In_xSb$  as well as behavior previously reported for  $Ga_{1-x}In_xAs$ <sup>2</sup> and  $K_{1-x}Rb_xI$ .<sup>5</sup>

#### ACKNOWLEDGMENTS

The authors wish to acknowledge helpful discussions with Professor E. Burstein, University of Pennsylvania; Professor E. Montroll, University of Rochester; Dr. H. Scher and Dr. T. Hayes of Xerox Corporation; and Dr. K. Weiser of IBM.

<sup>†</sup>A preliminary version of this paper was presented at the March, 1970 APS meeting [Bull. Am. Phys. Soc. **15**, 382 (1970)].

<sup>1</sup>G. Lucovsky, M. H. Brodsky, and E. Burstein, in *Localized Excitations in Solids*, edited by R. F. Wallis (Plenum, New York, 1968), p. 592.

<sup>2</sup>M. H. Brodsky and G. Lucovsky, Phys. Rev. Letters **21**, 990 (1968).

<sup>3</sup>See, for example, A. S. Barker, Jr., and H. W. Verleur, Solid State Commun. **5**, 695 (1967).

<sup>4</sup>F. Kruger, O. Reinkober, and E. Koch-Holm, Ann. Physik **85**, 110 (1928).

<sup>5</sup>J. H. Fertel and C. H. Perry, Phys. Rev. **184**, 874 (1969).

<sup>6</sup>R. M. Fuller, C. M. Randall, and D. J. Montgomery, Bull. Am. Phys. Soc. **9**, 644 (1964); also R. M. Fuller, Ph. D. thesis, Michigan State University, 1965 (unpublished).

<sup>7</sup>P. J. Gielisse, J. N. Pendl, L. C. Mansur, R. Marshall, S. S. Mitra, R. Mykolajewycz, and A. Smakula, J. Appl. Phys. **36**, 2446 (1965).

<sup>8</sup>G. Lucovsky, E. Lind, and E. A. Davis, in *II-VI Semiconducting Compounds*, edited by D. G. Thomas (Benjamin, New York, 1967), p. 1150.

<sup>9</sup>I. F. Chang and S. S. Mitra, Phys. Rev. **172**, 924 (1968).

<sup>10</sup>H. W. Verleur and A. S. Barker, Jr., Phys. Rev.

**149**, 715 (1966).

<sup>11</sup>Y. S. Chen, W. Shockley, and G. L. Pearson, Phys. Rev. **151**, 648 (1966).

<sup>12</sup>M. Balkanski, R. Beserman, and J. M. Besson, Solid State Commun. **4**, 201 (1966).

<sup>13</sup>D. W. Langer, Y. S. Park, and R. N. Euwema, Phys. Rev. **152**, 788 (1966).

<sup>14</sup>H. W. Verleur and A. S. Barker, Jr., Phys. Rev. **155**, 750 (1967).

<sup>15</sup>J. F. Parrish, C. H. Perry, O. Brafman, I. F. Chang, and S. S. Mitra, in *II-VI Semiconducting Compounds*, edited by D. G. Thomas (Benjamin, New York, 1967), p. 1164.

<sup>16</sup>M. Hegems and G. L. Pearson, Phys. Rev. B **1**, 1576 (1970).

<sup>17</sup>W. G. Spitzer and D. A. Kleinman, Phys. Rev. **121**, 1324 (1961).

<sup>18</sup>G. Lucovsky, M. H. Brodsky, and E. Burstein, preceding article, Phys. Rev. B **2**, 3295 (1970); Bull. Am. Phys. Soc. **15**, 382 (1970).

<sup>19</sup>F. Matossi, J. Chem. Phys. **19**, 161 (1951).

<sup>20</sup>Note added in proof. The expected mode occurrence for  $GaAs_{1-x}Sb_x$  and  $InAs_{1-x}Sb_x$  has recently been reported by G. Lucovsky and M. F. Chen [Solid State Commun. **8**, 1397 (1970)]. They also confirmed that  $Ga_{1-x}In_xAs$  is representative of category (2) behavior.